



ELSEVIER

Available online at [www.sciencedirect.com](http://www.sciencedirect.com)

SCIENCE @ DIRECT®

Optics Communications 249 (2005) 319–328

OPTICS  
COMMUNICATIONS

[www.elsevier.com/locate/optcom](http://www.elsevier.com/locate/optcom)

# Surface and bulk absorption in $\text{CaF}_2$ at 193 and 157 nm

Ch. Görling\*, U. Leinhos, K. Mann\*

*Laser-Laboratorium Göttingen, Hans-Adolf-Krebs-Weg 1, D-37077 Göttingen, Germany*

Received 21 September 2004; received in revised form 17 January 2005; accepted 20 January 2005

## Abstract

Comprehensive calorimetric absorption measurements were performed for  $\text{CaF}_2$  crystals at irradiation wavelengths 193 and 157 nm. By using samples with different thickness a separation of surface and bulk absorptance could be achieved and thus, single- and two-photon absorption coefficients could be determined for both wavelengths. For the surface absorptance, a dependence of the polishing grade of the sample was observed at 193 nm. The investigation of earlier reported repetition rate dependencies of the effective two-photon absorption coefficient at 193 nm was extended up to a repetition rate of 2.8 kHz. In contrast to the measurements at 193 nm, no such dependence at all could be found at 157 nm. Both results support already proposed models of the absorption mechanisms in wide band-gap materials.

© 2005 Elsevier B.V. All rights reserved.

*PACS:* 42.70.-a; 42.87.-d; 78.20.Ci; 42.65; 61.80.Az

*Keywords:* DUV/VUV laser calorimetry;  $\text{CaF}_2$ ; Single- and two-photon absorption coefficients; Surface and bulk absorption; Next generation lithography

## 1. Introduction

According to the roadmap of the Semiconductor Industry Association (SIA) [1], the deployment

of the ArF excimer laser wavelength 193 nm (DUV) for microlithography is already on the way. By using this wavelength, feature sizes down to 65 nm can be generated already with conventional exposure techniques, and with the recent introduction of immersion techniques the use of ArF and/or  $\text{F}_2$  lasers will allow to obtain even much smaller features. Immersion lithography is considered to be principally suitable for the 32 nm node and thus could make alternative techniques such as nanoimprint or EUV unnecessary,

\* Corresponding authors. The author is now with the Volkswagen AG, Brieffach 1653, D-38436 Wolfsburg, Germany. Tel.: +49 5361 9 49998 (Ch. Görling); Tel.: +49551503541; fax: +49551503599 (K. Mann).

*E-mail addresses:* [christian.goerling@volkswagen.de](mailto:christian.goerling@volkswagen.de) (Ch. Görling), [kmann@llg.gwdg.de](mailto:kmann@llg.gwdg.de) (K. Mann).

especially since the latter has still to overcome a lot of technical problems and is expected to be extremely cost-intensive.

In the DUV and VUV spectral range, however, there are only a few wide band-gap optical materials with acceptable transmission, i.e., besides fused silica, essentially the alkaline earth fluorides. Especially  $\text{CaF}_2$  is considered as the most promising candidate for lithography due to its high transmission, chemical and physical stability and its small birefringence at 193 and 157 nm [2]. In the past, calorimetric absorption measurements on  $\text{CaF}_2$  crystals at 193 nm were performed [3,4] and extended to 157 nm [5,6]. Linear and nonlinear absorption coefficients were determined and appropriate models for the absorption mechanisms could be derived. However, it was not possible to separate surface and bulk absorption in these experiments. Alternatively to laser calorimetry, absorptance can also be measured by employing laser-induced deflection techniques (LID) [7,8,15]. With LID, however, only bulk properties can be investigated, and an absolute calibration of  $\text{CaF}_2$  data is difficult.

In general, besides linear absorption from the surface and defect states within the forbidden zone, two-photon absorption of laser radiation is also possible at 193 and 157 nm in  $\text{CaF}_2$  due to the band-gap of about 12 eV [9], which is smaller than twice the photon energy of 12.42 eV (193 nm) and 15.9 eV (157 nm), respectively. Consequently, absorptance of  $\text{CaF}_2$  crystals depends on a variety of parameters, and Lambert–Beer’s law for surface, single- and two-photon absorption can be written as

$$\begin{aligned} A(\lambda, d, H, \Delta t, \sigma_{\text{rms}}) &= \left| \frac{dI}{I} \right| \\ &= A_{\text{surf}}(\lambda, \sigma_{\text{rms}}) \\ &\quad + \left( \alpha(\lambda) + \beta_{\text{eff}}(\lambda, \Delta t) \frac{H}{\tau} \right) d. \end{aligned} \quad (1)$$

Here,  $A$  denotes the total absorptance;  $A_{\text{surf}}$ , the surface absorptance;  $\alpha_0$  and  $\beta_{\text{eff}}$ , are the single- and effective two-photon absorption coefficients, respectively;  $d$ , the sample thickness;  $\sigma_{\text{rms}}$ , the surface roughness;  $\lambda$ , the irradiation wavelength;  $\Delta t$ ,

the time interval between laser pulses;  $H$ , the fluence and  $\tau$ , the pulse length.

As previous investigations have shown,  $\alpha_0$  and  $\beta_{\text{eff}}$  are quantities which depend on the concentration of crystal defects; especially  $\beta_{\text{eff}}$  summarizes pure two-photon absorption ( $\beta$ ) and two-step absorption via defect states ( $\beta_{2\text{-step}}$ ). Since  $\beta \ll \beta_{2\text{-step}}$ , laser calorimetry detects to a large extent the influence of impurities or defects [5].

An important question is the fraction of surface absorption  $A_{\text{surf}}$  in relation to bulk absorption. According to Eq. (1) it is obviously possible to separate both by measurement of total absorption  $A$  for samples with different thickness  $d$ , provided that the crystals have the same  $\alpha$  and  $\beta_{\text{eff}}$ . In practice, they should stem from the same mother crystal and therefore have similar defect concentrations, and, moreover, the same surface finish ( $A_{\text{surf}}$ ).

In this paper, the separation of surface and bulk absorption in  $\text{CaF}_2$  for 193 and 157 nm is demonstrated for the first time. Furthermore, an influence of the surface roughness on the linear absorption  $A_0$  at 193 nm was found and investigated in detail. Due to the great importance of the absorption behaviour at high repetition rates for the microlithographic process, the previously observed repetition rate dependence of two-photon absorption at 193 nm between 25 and 300 Hz [4] was extended to rates up to 2.8 kHz at 193 nm and also studied up to 150 Hz at 157 nm. The results are discussed in terms of a simple model, proposed already in [4].

## 2. Experimental set-up

Absorptance measurements are performed at 193 and 157 nm according to ISO 11551 [11], using DUV and VUV absorption calorimeters already described earlier [4,5,10]. The experimental set-up of the high repetition rate DUV calorimeter was in principle the same as in [10], Fig. 1. Here, an ArF excimer laser (Lambda Physik, Novaline A4020) served as a light source with maximum repetition rates of 2.8 kHz (continuous mode) and 4 kHz (burst mode), respectively, and with a pulse length of 22.7 ns (integral square

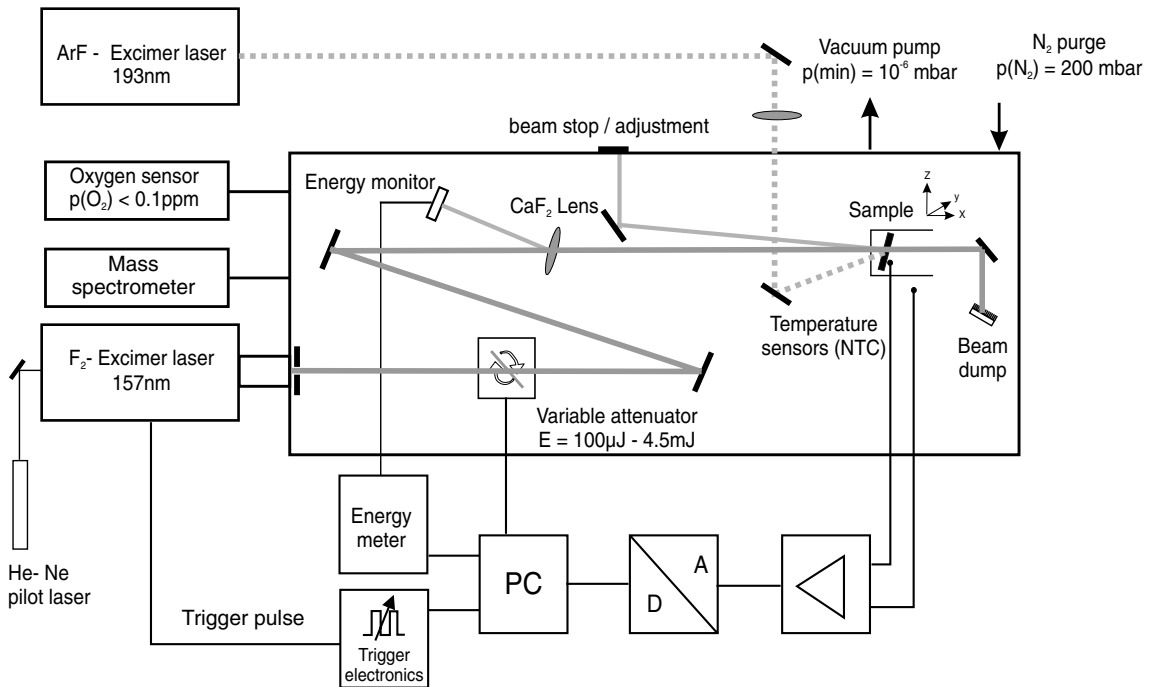


Fig. 1. The VUV absorption calorimeter. After thermal equilibration, the sample is irradiated with a burst of laser pulses, and the temperature increase  $\Delta T$  is detected by the temperature sensor (NTC). Measuring the total irradiation energy  $Q_{\text{in}}$  by an energy monitor at the same time, the absorptance is given by  $A = c_{\text{eff}} \cdot \Delta T / Q_{\text{in}}$ . The effective heat capacity  $c_{\text{eff}}$  of the sample is determined in a separate experiment by electrical heating.

value). The laser fluence on the sample could be varied between 10 and 50  $\text{mJ}/\text{cm}^2$ . Fig. 1 depicts the VUV absorption calorimeter schematically. The whole optical arrangement is embedded into a UHV chamber with a high purity  $\text{N}_2$  atmosphere (Nitrogen 6.0). In order to minimize the influence of contaminations on the temperature signal, several pump and purge cycles are carried out. For a reduction of scattered light by the  $\text{N}_2$  atmosphere, the  $\text{N}_2$  pressure is kept constant at 200 mbar during the measurements. The oxygen content is less than 0.1 ppm, and only a very small water content (partial pressure about  $4 \times 10^{-8}$  mbar) could be detected by mass spectrometry. A variable attenuator inside the optical path allowed for fluence variations between 5 and 100  $\text{mJ}/\text{cm}^2$ . The pulse duration was 23.4 ns (integral square) [12].

Prior to the actual measurements, the samples were pre-irradiated in air at 193 nm and total

doses of 8  $\text{kJ}/\text{cm}^2$  (conditioning, laser cleaning [28–30]). During an absorption measurement cycle, the samples were irradiated for 15 s (193 nm) and 75 s (157 nm), respectively.

### 3. Results and discussion

#### 3.1. Separation of surface and bulk absorption at 193 and 157 nm

For separation of surface and bulk absorption a series of cylindrical  $\text{CaF}_2$  samples (diameter 25 mm, thicknesses 0.2, 0.4 and 0.6 cm) was cut from the same high purity crystal in (111) direction and polished until a surface roughness  $\sigma_{\text{rms}}$  of 0.66 nm was reached. Fluence dependent absorptance measurements were performed at 193 and 157 nm. Fig. 2 summarises the results for both wavelengths.

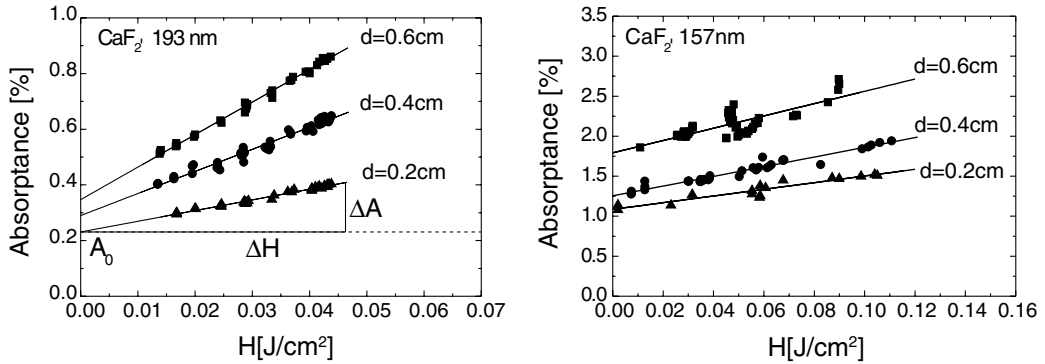


Fig. 2. Absorbance as a function of fluence  $H$  for  $\text{CaF}_2$  samples with different thicknesses at 193 nm (left) and 157 nm (right). The linear absorbance  $A_0$  is given by the intercept with the ordinate while the nonlinear absorbance is represented by the product of slope (nonlinear absorbance term  $B$ ) times fluence ( $\Delta A/\Delta H \cdot H = B \cdot H$ ).

As seen from Fig. 2, a linear dependence of the absorbance  $A$  on fluence  $H$  is found at both wavelengths and can be written as

$$A(d, H) = A_0(d) + \frac{\Delta A(d)}{\Delta H} \cdot H = A_0(d) + B(d) \cdot H. \quad (2)$$

The linear absorbance  $A_0$  is given by the intercept with the ordinate and depends on the crystal thickness, as well as the nonlinear absorbance term  $B$ , which can be derived from the slope. At 157 nm, the scattering of the absorbance values is considerably larger. This can be attributed to contamination

on the sample surface ( $\text{H}_2\text{O}$ ,  $\text{C}_n\text{H}_m$ ) which affect the temperature signal.

In Fig. 3, the linear absorbance  $A_0(d)$  and the product of nonlinear absorbance and pulse length  $B \cdot \tau$  is plotted against the sample thickness. In the case of 193 nm, a very good linear correlation is found. From the slope, the single-photon absorption coefficient  $\alpha$  can be derived, which amounts to  $2.89 \times 10^{-3} \text{ cm}^{-1}$ . Extrapolation to thickness zero yields a surface absorbance  $A_{\text{surf}}$  of 0.17% for both surfaces. Therefore, surface absorbance dominates the linear absorbance up to a crystal thickness of about 6 mm.

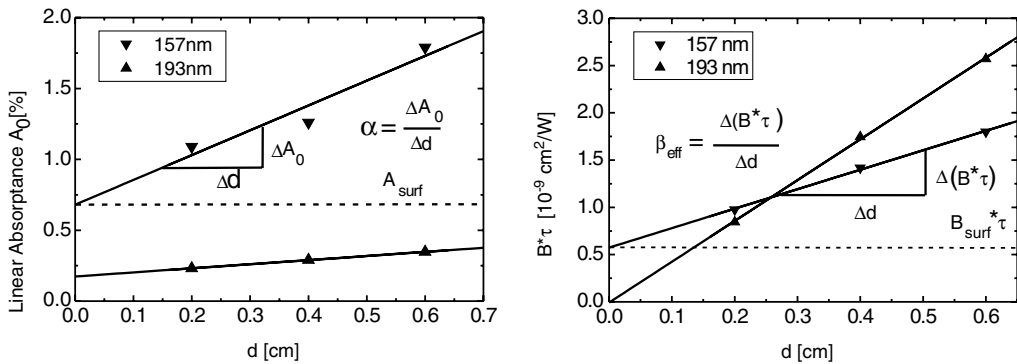


Fig. 3. (Left) Linear absorbance  $A_0$  vs. sample thickness  $d$ ; the surface absorbance  $A_{\text{surf}}$  is given by the intercept with the ordinate, the single-photon absorbance  $\alpha \cdot d$  by the slope of the straight lines. (Right) Product of nonlinear absorbance term and pulse length ( $B \cdot \tau$ ) versus sample thickness  $d$ . The effective two-photon absorption coefficient  $\beta_{\text{eff}}$  is given by the slope. Notice the nonvanishing term  $B \cdot \tau$  at thickness zero for 157 nm, indicating a contribution of the surface to the two-photon absorption ( $B_{\text{surf}} \cdot \tau > 0$ ).

The linear absorptance at 157 nm also follows a linear trend. Here, a significantly larger  $\alpha$  of  $17.5 \times 10^{-3} \text{ cm}^{-1}$  is determined, resulting from the excitation closer to the conduction band. The surface absorption (0.68 %) is also a factor of four higher than at 193 nm. Obviously, surface states are excited here at a progressive rate. Both absorption values at 157 nm agree well with already published data derived from transmission measurements [13].

The product  $B \cdot \tau$ , depicted in Fig. 3(right), shows a good linear dependence on the sample thickness at both wavelengths. Here, the slope represents the effective two-photon absorption coefficient  $\beta_{\text{eff}}$ . As published already earlier [5], the two-photon absorption at 193 nm is found to be more than a factor of 2 higher than at 157 nm (193 nm:  $\beta_{\text{eff}} = 4.31 \times 10^{-9} \text{ cm/W}$ , 157 nm:  $\beta_{\text{eff}} = 2.06 \times 10^{-9} \text{ cm/W}$ ). This interesting experimental fact can be explained by resonant excitation of electrons from defect states near the valance band into the conduction band at 193 nm, since the band gap of  $\text{CaF}_2$  (11.5–12 eV) corresponds well to twice the photon energy (12.82 eV). At 157 nm, however, the two-photon energy (15.8 eV) exceeds the vacuum energy, and thus only a small two-photon absorption is measured.

For 193 nm, the product  $(B \cdot \tau)(d)$  crosses exactly the origin, indicating that two-photon absorption is a pure bulk effect. At 157 nm, however, an intercept with the ordinate of  $B_{\text{surf}} = 5.74 \times 10^{-10} \text{ cm}^2/\text{W}$  is evident. This unexpected nonlinear absorption of the surface at 157 nm suggests the existence of a thin interface layer with another chemical composition than the  $\text{CaF}_2$  bulk material. Earlier reported absorptance measurements of thin  $\text{Al}_2\text{O}_3$  films at 193 nm also showed a nonnegligible two-photon absorption [14], whereas at 248 nm no nonlinear absorption could be observed at all [16]. This behaviour was explained by resonant excitation of virtual colour centres inside the film at 193 nm. Probably, similar colour centres or defect states inside the interface layer of the  $\text{CaF}_2$  samples are excited at 157 nm, but not at 193 nm.

Table 1 summarises the absorption coefficients for the set of  $\text{CaF}_2$  crystals at both wavelengths.

### 3.2. Roughness dependence of surface absorption at 193 nm

For a better statistical basis another set of eight  $\text{CaF}_2$  samples with various thicknesses was produced from the same mother crystal and the absorptance data were determined as described in Section 3.1. The results for  $A_0$  and  $\beta_{\text{eff}}$  are displayed in Fig. 4. The obtained linear correlations are again quite good, and the evaluation yields  $\alpha = 5 \times 10^{-3} \text{ cm}^{-1}$ ,  $A_{\text{surf}} = 0.24\%$  (both surfaces), and  $\beta_{\text{eff}} = 1.56 \times 10^{-9} \text{ cm/W}$ . Obviously, there are two samples with deviating values of linear absorption; however, their  $\beta_{\text{eff}}$  values agree well with those of the other samples (hollow circles in Fig. 4), confirming the fact that samples from the same crystal have the same bulk defect concentration.

Thus, the reason for the deviation in  $A_0$  clearly is a surface effect, as could be confirmed by roughness measurements using an atomic force microscope (Nanoscope, Digital Instruments): the crystals with deviating  $A_0$  ( $d = 2.25$  and  $4.5 \text{ mm}$ ) showed much higher  $\sigma_{\text{rms}}$  values (2.0 and 2.66 nm) than the other samples (0.86 to 1.83 nm). Moreover, absorptance measurements of two samples with different polishing grades from another mother crystal showed the same result (cf. Fig. 5): while  $\beta_{\text{eff}}$  amounts to  $7.5 \times 10^{-9} \text{ cm/W}$  in both cases, the linear absorption  $A_0$  (intercept with the ordinate) reduces from 1.24% to 0.56% due to a decrease of surface roughness by a factor of 10 (3.73 and 0.335 nm, respectively).

The drastic decrease of linear absorptance with improved surface finish was investigated systematically by repeated determination of  $A_0$  for a single  $\text{CaF}_2$  sample after successive polishing steps (cf.

Table 1

Effective single-photon, two-photon and surface absorption coefficients, as determined for a set of  $\text{CaF}_2$  crystals with different thicknesses and a surface roughness of 0.66 nm

Excitation wavelength	193 nm	157 nm
$\tau$ (int.squ.) [ns]	22.7	23.4
$\alpha$ [ $10^{-3} \text{ cm}^{-1}$ ]	2.89	17.5
$\beta_{\text{eff}}$ [ $10^{-9} \text{ cm/W}$ ]	4.31	2.06
$A_{\text{surf}}$ [%]	0.17	0.68
$B_{\text{surf}} \cdot \tau$ [ $10^{-9} \text{ cm}^2/\text{W}$ ]	0	0.574

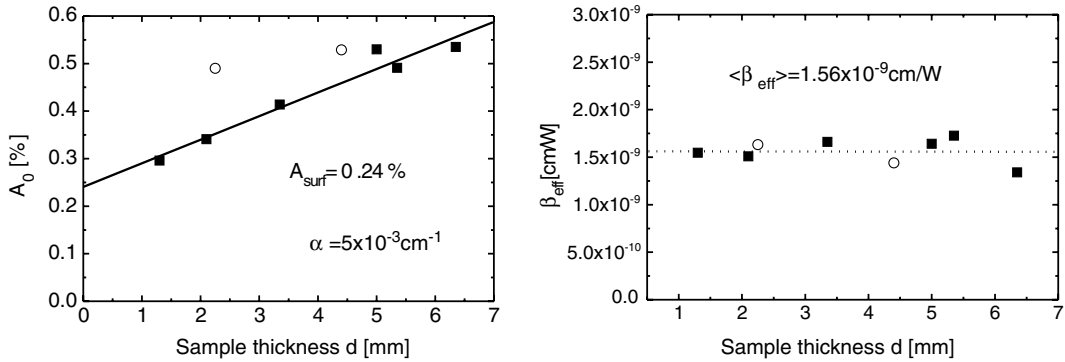


Fig. 4. (Left) Linear absorbance for eight  $\text{CaF}_2$  crystals of different thickness. The two deviating absorbance values (hollow circles) were not considered for evaluation of  $A_{\text{surf}}$  and  $\alpha$ . (Right) The effective two-photon absorption coefficient  $\beta_{\text{eff}}$  is nearly constant for all samples.

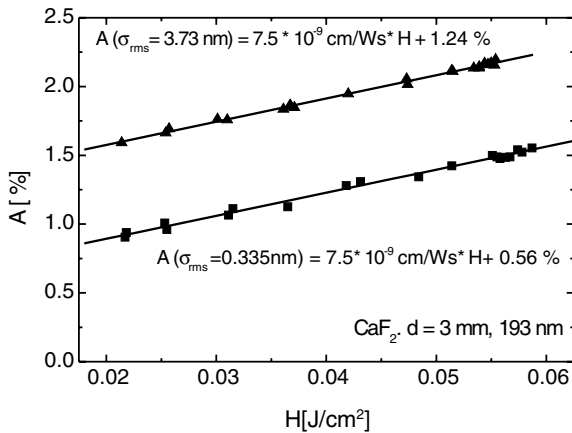


Fig. 5. Absorbance vs. fluence for two  $\text{CaF}_2$  samples ( $d = 3$  mm, same crystal, 300 Hz) with different surface finish. The linear absorbance reduces from 1.24% to 0.56% for decreasing surface roughness from 3.73 to 0.335 nm, whereas the effective two-photon absorption coefficient is the same in both cases ( $7.5 \times 10^{-9}$  cm/W).

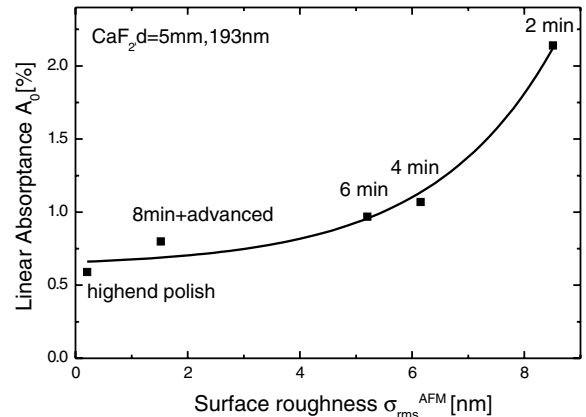


Fig. 6. Linear absorbance as a function of surface roughness for a progressively smoothed  $\text{CaF}_2$  sample. The indicated time corresponds to the duration of a diamond polish procedure. For the advanced ( $\sigma_{\text{rms}} = 1.52$  nm) and high-end polish ( $\sigma_{\text{rms}} = 0.21$  nm) special techniques were used. The fit represents a single exponential decay and results in a linear absorbance of about 0.6% for two ideal surfaces of the sample.

Fig. 6). The linear absorbance decreases nearly exponentially with decreasing surface roughness. At zero roughness, i.e., for an ideal surface, a linear absorbance of about 0.6% can be extrapolated for both surfaces of this sample. Since this value is reached already at the smallest roughness of 0.2 nm, no further improvement is expected from additional polishing.

We interpret the observed roughness dependence of absorption by the fact, that more contaminants (e.g., water and hydrocarbons) can be

adsorbed on a surface with larger roughness. The adsorption of a stable monolayer of water was demonstrated by UPS experiments even for well polished  $\text{BaF}_2$  and  $\text{CaF}_2$  crystals [17]. Second, UPS measurements also gave evidence that oxygen or  $\text{OH}^-$  leads to a maximum of the electronic density of states up to 6 eV above the valence band [18], which could be simulated theoretically by Hartree–Fock methods [19]. A reduction of this oxygen-induced density of states was shown for

diamond polished as compared to standard polished samples [20]. Obviously, a possible interface layer on the surface consisting of CaO/Ca(OH)<sub>2</sub> is strongly reduced by progressive smoothing. For the super-polished samples ( $\sigma_{\text{rms}} < 0.5$  nm) it is furthermore conceivable that roughness-induced surface states in the band gap caused by point defects (e.g., surface F-centres) are reduced by polishing. The existence of such surface defect states was demonstrated in BaF<sub>2</sub> by multiphoton ionization and desorption experiments [21]. Especially, there are indications for an important role of surface defects for radiation-damage processes in wide band gap materials [22–24]. In summary, the surface-induced two-photon absorption at 157 nm as well as the roughness dependence of linear absorption at 193 nm are strong indications for the existence of an absorbing interface layer on the surface of CaF<sub>2</sub> crystals.

### 3.3. Repetition rate dependence of bulk absorption at 193 and 157 nm

In an earlier paper [4] a dependence of the nonlinear bulk absorption  $\beta_{\text{eff}}$  from the laser repetition rate  $f_{\text{rep}}$  was observed for CaF<sub>2</sub> samples with a certain defect concentration (193 nm,  $f_{\text{rep}} < 300$  Hz) which was found to be strongly nonlinear for samples with large  $\beta_{\text{eff}}$ . These investigations were now

extended to repetition rates of up to 2.8 kHz for two representative CaF<sub>2</sub> samples labeled A and F in [4] with high ( $13 \times 10^{-9}$  cm/W) and low ( $2 \times 10^{-9}$  cm/W)  $\beta_{\text{eff}}$  value at 300 Hz, respectively. Fig. 7(left) shows the first repetition rate dependent absorptance measurement up to 2.8 kHz. It is evident that the strong nonlinear increase in absorptance with increasing repetition rate continues up to 2.8 kHz, showing no indication of saturation.

This behaviour can be explained by the model of transient states proposed in [4] (cf. Fig. 9). Here, besides pure two-photon absorption and two-step absorption within the same laser pulse via defect states, also two-step absorption by occupation of long living transient states within consecutive pulses is assumed. These processes lead, in summary, to the following repetition rate dependence of the effective two-photon absorption coefficient:

$$\beta_{\text{eff}}(\Delta t) = \frac{\sigma\eta\sigma_{\text{D}}[D]\tau}{\hbar\omega} \left( \frac{2}{1 - \exp(-\Delta t/\tau_{\text{L}})} - 1 \right) + \beta, \quad (3)$$

where  $\sigma$  and  $\sigma_{\text{D}}$  denote the absorption cross-sections for the first and second absorption step;  $\eta$ , the efficiency of formation of occupied defect levels;  $[D]$ , the defect concentration;  $\tau$ , the pulse length and  $\tau_{\text{L}}$ , the lifetime of the transient state.

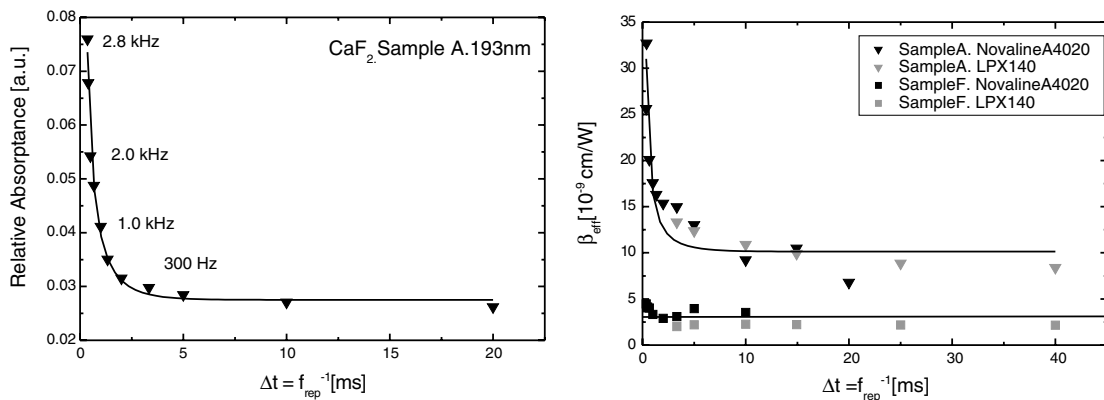


Fig. 7. (Left) Relative absorptance of sample A as a function of the time between consecutive pulses  $\Delta t = f_{\text{rep}}^{-1}$  (laser fluence  $33 \text{ mJ/cm}^2$ ) with a fit according to Eq. (3). (Right) Effective two-photon absorption coefficients for repetition rates up to 300 Hz (LPX 140, grey) and 2.8 kHz (A4020, black), respectively. From the fit on the data of sample A, a  $\tau_{\text{L}}$  of about 2 ms can be derived. For sample F the averaged  $\beta_{\text{eff}}$  (continuous line) amounts to  $3.1 \times 10^{-9}$  cm/W.

The relative (left) and absolute  $\beta_{\text{eff}}$  data (right) of samples A and F shown in Fig. 7 can be fitted nicely by Eq. (3), yielding a lifetime of the transients of about 2 ms. For comparison, the earlier reported data [4] are enclosed. Both series correspond to each other within the experimental error. From Fig. 7(right) it is also striking, that the high quality crystal (sample F) reveals a nearly constant  $\beta_{\text{eff}}$  for varying repetition rate.

The observed long lifetime in the millisecond range suggests the formation of colour centres, as known e.g., from doped crystals [25]. However, also energy transfer reactions on this time scale are conceivable. In order to clarify the nature of the transients, additional techniques like spectroscopy (radiatively decaying defects), gamma diffractometry (dislocations) and laser induced bulk damage threshold measurements were performed on crystals with different defect concentrations ( $\beta_{\text{eff}}$ ) [6]. However, no correlation at all could be found. Thus, the transient states can be attributed to statistically distributed point defects inside the crystal which are decaying nonradiatively. Their long lifetime and the fact that they cannot be excited at 157 nm suggest that these defects are represented by

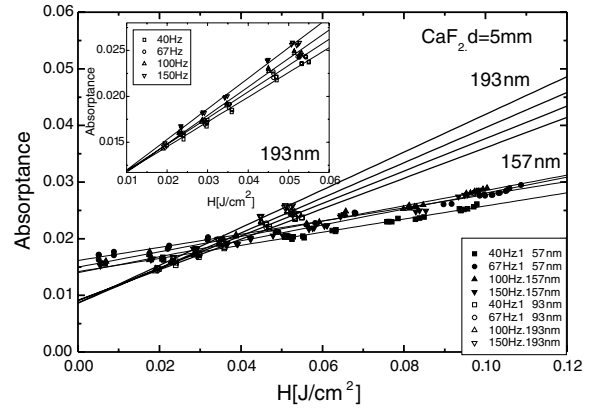


Fig. 8. Absorbance of a  $\text{CaF}_2$  sample as a function of fluence for irradiation wavelengths 193 and 157 nm and repetition rates between 40 and 150 Hz. The inset displays the enlarged 193 nm data.

sharp energetic levels in the middle of the energy gap ( $\approx 6$  eV). This would be consistent with a large electron binding energy (“deep defects”, [26,27]).

For comparison, the repetition rate dependence of the two-photon absorption observed at 193 nm was also investigated at 157 nm. In Fig. 8 respective absorption measurements of a  $\text{CaF}_2$  sample

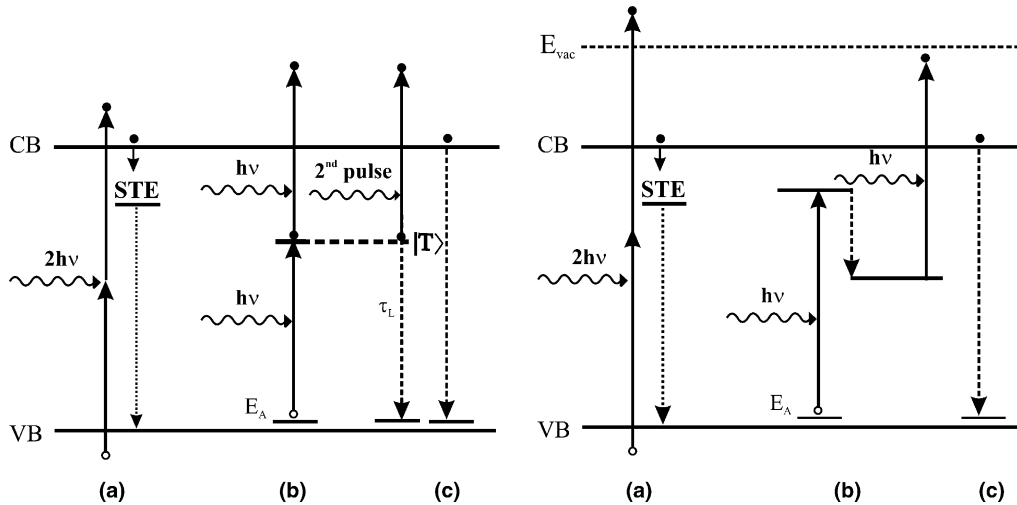


Fig. 9. Two-photon absorption processes at 193 nm (left) and at 157 nm (right). Two-photon absorption leads in both cases to the formation of self-trapped excitons (STE), which decay radiatively and nonradiatively (a). (Left) With the photon energy of 6.42 eV (193 nm), a resonant excitation of defect states (two-step absorption, (b)) and related long living transient states (c) is possible. (Right) Due to the higher photon energy of 7.9 eV, and therefore non existing conduction band states at 157 nm, two-step absorption is only possible indirectly by relaxation into energetically lower defect levels (b). At both wavelengths, a relaxation of conduction band electrons into the origin acceptor level  $E_A$  takes place, leading to heating of the crystal (c).

with a large number of defect states are compiled for both wavelengths. The effective two-photon absorption at 193 nm (=slope of straight lines) again increases with growing repetition rates, whereas it remains nearly constant at 157 nm. Moreover, as shown in Section 3.1 and in [5], the absorption measured at 157 nm exhibits a much weaker two-photon absorption behaviour than at 193 nm. At a critical fluence of  $35 \text{ mJ/cm}^2$  there is a crossing between the two curves; thus, beyond this fluence the absorption at 157 nm is lower than at 193 nm.

These experimental data can be interpreted using the energy level diagrams in Fig. 9. While for 193 nm besides two-step absorption long living transient states can be resonantly excited, followed by absorption of a second photon from successive laser pulses (Fig. 9(left)) [4], at 157 nm another kind of two-step absorption is assumed, which takes place within the same laser pulse: By the first photon the acceptor electrons near the valence band are promoted into defect states near the conduction band, followed by a relaxation into lower defect levels, from which they can be excited into the conduction band by absorption of a second photon. Of course it is conceivable that the defect and transient states in the middle of the band gap can be resonantly excited at 193 nm only due to the appropriate photon energy and fulfilled dipole selection rules, while for 157 nm photons corresponding states do not exist. However, the fact of different two-photon absorption coefficients for various  $\text{CaF}_2$  samples at 157 nm [5] is a strong indication for the existence of such defect states and a related two-step absorption mechanism. Finally, the absence of a distinct repetition rate dependence of  $\beta_{\text{eff}}$  at 157 nm also supports the indirect absorption mechanism.

#### 4. Summary and conclusion

In this paper, comparative calorimetric absorption measurements on  $\text{CaF}_2$  at 193 and 157 nm were presented. For both irradiation wavelengths a separation of surface and bulk absorptance was achieved by using samples with different thicknesses. As the main result, absolute values for

the surface and the bulk absorptance (single and two-photon absorption coefficients) could be given.

For thin samples ( $d < 6 \text{ mm}$ ), surface absorption clearly dominates the total absorptance. For 157 nm the single-photon absorption  $\alpha$  and the surface absorption  $A_{\text{surf}}$  are higher than at 193 nm due to the excitation closer to the band edge. On the other hand, the two-photon absorption is significantly smaller at 157 nm, since  $2h\nu_{157 \text{ nm}}$  exceeds already the vacuum level. The high surface absorption at 157 nm with a nonlinear contribution is a strong indication for the existence of a thin absorbing interface layer. The surface absorptance at 193 nm depends nearly exponentially on the surface roughness, which is explained by the reduction of the interface layer by improved polishing.

The bulk absorptance shows a strong repetition rate dependence up to 2.8 kHz for samples with high  $\beta_{\text{eff}}$  values, indicating a dominant role of defect induced two-step absorption at high repetition rates; thus, for applications as e.g., microlithography only  $\text{CaF}_2$  crystals with highest quality can be used. A repetition rate dependence of  $\beta_{\text{eff}}$  is not observed at 157 nm. Both effects could be explained in terms of a simple model, where transient defect states enhance the two-step absorption at 193 nm, while at 157 nm an indirect absorption mechanism takes place. In order to improve the model presented above, further investigations are necessary.

#### Acknowledgements

The authors thank the Bundesministerium für Bildung und Forschung for financial support within the EUREKA project CHOCLAB II (EU 2359). The cooperation with the crystal manufacturers Korth Kristalle, Kiel (Germany) and Schott Lithotec AG, Jena (Germany) is gratefully acknowledged.

#### References

- [1] ITRS International Technology Roadmap for Semiconductors, International Sematec. Available from: <[www.Sematech.org/public](http://www.Sematech.org/public)>.

- [2] J.H. Burnett, Z.H. Levine, E.L. Shirley, *Phys. Rev. B* 64 (2001), p. 241102-1(R).
- [3] E. Eva, Dissertation Universität Göttingen, Cuvillier-Verlag, Göttingen, 2003. Download: <[www.cuvillier.de](http://www.cuvillier.de)>.
- [4] Ch. Görling, U. Leinhos, K. Mann, *Opt. Commun.* 216 (2003) 369.
- [5] Ch. Görling, U. Leinhos, K. Mann, *Appl. Phys. B* 74 (2002) 259.
- [6] Ch. Görling, Dissertation Universität Göttingen, Cuvillier-Verlag, Göttingen, 2003. Download: <[www.cuvillier.de](http://www.cuvillier.de)>.
- [7] M. Guntau, W. Triebel, *Rev. Sci. Instr.* 71 (2000) 2279.
- [8] B. Li, S. Martin, E. Welsch, *Opt. Lett.* 24 (1999) 1398.
- [9] G.W. Rubloff, *Phys. Rev. B* 5 (1972) 662.
- [10] E. Eva, K. Mann, *Appl. Phys. A* 62 (1996) 143.
- [11] ISO 11551, Test method for absorptance of optical laser components.
- [12] Dr. Voss, Lambda Physik AG, Private communication.
- [13] T.M. Bloomstein, M. Rothschild, R.R. Kunz, D.E. Hardy, R.B. Goodman, S.T. Palmacci, *J. Vac. Sci. Technol. B* 16 (1998) 3154.
- [14] O. Apel, K. Mann, A. Zoeller, R. Goetzelmann, E. Eva, *Appl. Opt.* 39 (2000) 3165.
- [15] U. Natura, C. Mühlig, W. Triebel, C. Görling, U. Leinhos, K. Mann, E. Eva, A. Pfeiffer, Instruments and standard test procedures for laser beam and optics characterization, Brochure to the final representation of the Eureka project EU-2359 (CHOCLAB II), 2003, p. 280.
- [16] Dr. U. Leinhos, Laser-Laboratorium Göttingen, Private communication, 2003.
- [17] J.C. Zink, J. Reif, E. Matthias, *Phys. Rev. Lett.* 68 (1992) 3595.
- [18] M. Reichling, M. Huisinga, S. Gogoll, C. Barth, *Surf. Sci.* 439 (1999) 181.
- [19] A.V. Puchina, V.E. Puchin, M. Huisinga, R. Bennowitz, M. Reichling, *Surf. Sci.* 402–404 (1998) 687.
- [20] M. Huisinga, Dissertation Freie Universität Berlin, 1998.
- [21] J. Reif, *Opt. Eng.* 28 (1989) 1122.
- [22] K. Tanimura, N. Itoh, *Nucl. Instr. Meth. B* 46 (1990) 207.
- [23] S. Gogoll, E. Stenzel, M. Reichling, H. Johansen, E. Matthias, *Appl. Surf. Sci.* 96–98 (1996) 332.
- [24] J.T. Dickinson, *Nucl. Instr. Meth. B* 91 (1994) 634.
- [25] M. Henke, J. Peršon, S. Kück, *J. Lumin.* 87–89 (2000) 1049.
- [26] H.J. Queisser, in: F. Sauter, O. Madelung, H.J. Queisser, J. Treusch (Eds.), *Advances in Solid State Physics*, vol. XI, F. Vieweg und Sohn, Braunschweig, since 1962 (2002: 42 vols).
- [27] S. Pantelides, in: F. Sauter, O. Madelung, H.J. Queisser, J. Treusch (Eds.), *Advances in Solid State Physics*, vol. XV, F. Vieweg und Sohn, Braunschweig, since 1962 (2002: 42 vols).
- [28] K. Mann, B. Wolff-Rottke, F. Müller, *Appl. Surf. Sci.* 96–98 (1996) 463.
- [29] N.S. McIntyre, R.D. Davidson, T.L. Walzak, R. Williston, M. Westscott, A. Pekarsky, *J. Vac. Sci. Technol. A* 9 (1991) 1355.
- [30] D.J. Krajnovich, M. Kulkarni, W. Leung, A.C. Tam, A. Spool, B. Yorck, *Appl. Opt.* 31 (1992) 6062.